

Simple nonlinearity evaluation and modeling of low-noise amplifiers with application to radio astronomy receivers

F. J. Casas, J. P. Pascual, M. L. de la Fuente, E. Artal, and J. Portilla

Citation: *Rev. Sci. Instrum.* **81**, 074704 (2010); doi: 10.1063/1.3463295

View online: <http://dx.doi.org/10.1063/1.3463295>

View Table of Contents: <http://rsi.aip.org/resource/1/RSINAK/v81/i7>

Published by the [American Institute of Physics](http://www.aip.org).

Related Articles

Controlling a telescope chopping secondary mirror assembly using a signal deconvolution technique
Rev. Sci. Instrum. **74**, 3802 (2003)

A wideband lag correlator for heterodyne spectroscopy of broad astronomical and atmospheric spectral lines
Rev. Sci. Instrum. **72**, 1531 (2001)

A medium-frequency interferometer for studying auroral radio emissions
Rev. Sci. Instrum. **71**, 3200 (2000)

Implementation of a photonic automatic gain control system for correcting gain variations in the Green Bank Telescope fiber optic system
Rev. Sci. Instrum. **71**, 3196 (2000)

The Mt. Fuji submillimeter-wave telescope
Rev. Sci. Instrum. **71**, 2895 (2000)

Additional information on *Rev. Sci. Instrum.*

Journal Homepage: <http://rsi.aip.org>

Journal Information: http://rsi.aip.org/about/about_the_journal

Top downloads: http://rsi.aip.org/features/most_downloaded

Information for Authors: <http://rsi.aip.org/authors>

ADVERTISEMENT



Simple nonlinearity evaluation and modeling of low-noise amplifiers with application to radio astronomy receivers

F. J. Casas,¹ J. P. Pascual,² M. L. de la Fuente,² E. Artal,² and J. Portilla³

¹*Physics Institute of Cantabria, CSIC-University of Cantabria, Av. Los Castros SN, 39005 Santander, Spain*

²*Department of Communications Engineering, University of Cantabria, 39005 Santander, Spain*

³*Department of Electricity and Electronics, University of the Basque Country, Apdo. 644, 48080 Bilbao, Spain*

(Received 27 April 2010; accepted 16 June 2010; published online 27 July 2010)

This paper describes a comparative nonlinear analysis of low-noise amplifiers (LNAs) under different stimuli for use in astronomical applications. Wide-band Gaussian-noise input signals, together with the high values of gain required, make that figures of merit, such as the 1 dB compression (1 dBc) point of amplifiers, become crucial in the design process of radiometric receivers in order to guarantee the linearity in their nominal operation. The typical method to obtain the 1 dBc point is by using single-tone excitation signals to get the nonlinear amplitude to amplitude (AM-AM) characteristic but, as will be shown in the paper, in radiometers, the nature of the wide-band Gaussian-noise excitation signals makes the amplifiers present higher nonlinearity than when using single tone excitation signals. Therefore, in order to analyze the suitability of the LNA's nominal operation, the 1 dBc point has to be obtained, but using realistic excitation signals. In this work, an analytical study of compression effects in amplifiers due to excitation signals composed of several tones is reported. Moreover, LNA nonlinear characteristics, as AM-AM, total distortion, and power to distortion ratio, have been obtained by simulation and measurement with wide-band Gaussian-noise excitation signals. This kind of signal can be considered as a limit case of a multitone signal, when the number of tones is very high. The work is illustrated by means of the extraction of realistic nonlinear characteristics, through simulation and measurement, of a 31 GHz back-end module LNA used in the radiometer of the QUIJOTE (Q U I JOint TENERife) CMB experiment. © 2010 American Institute of Physics. [doi:10.1063/1.3463295]

I. INTRODUCTION

In the design process of radiometric receivers,¹ linearity is one of the main goals to be achieved.²⁻⁵ In these receivers there are two main sources of nonlinear behavior: detectors and low-noise amplifiers (LNAs). Linearity of astronomical detectors is considered an important issue.⁶⁻¹¹ In the particular case of LNAs, linearity is used to be defined by taking into account a figure of merit such as the 1 dBc point and setting an appropriate input power back-off level. This point is part of the nonlinear amplitude to amplitude (AM-AM) characteristic, typically estimated by means of single-tone excitation signals. Nevertheless, there are many applications in which the operation of the circuits is driven by wide-band excitation signals. This is the case of radiometric receivers where the excitation signal comes from the sky in the form of a wide-band Gaussian-noise signal to be filtered and amplified in the band of interest. As will be shown in this work, the different nature of this kind of excitation signal, with respect to the typical one-tone test signal, makes the receiver LNAs present a more nonlinear behavior than it would be expected for the single-tone nonlinear characteristics.¹² In fact, similar nonlinear effects have been detected in power amplifiers of communication systems with wide-band-modulated excitation signals.¹³ So, in order to analyze the

suitability of the LNAs' nominal operation point, linearity figures of merit, such as the 1 dBc point, have to be obtained, but using realistic excitation signals.

This paper is focused on the extraction of the nonlinear characteristics of a 31 GHz LNA that is part of the radiometric receiver for the QUIJOTE CMB experiment.¹⁴ An analytical study of compression effects due to amplifier excitation signals composed of several tones is proposed. On the other hand, nonlinear characteristics with wide-band Gaussian-noise excitation signals are obtained by simulation and measurement. This kind of signal can be considered as a limit case of a multitone signal with a very high number of tones. Due to the intermodulation noise, the nonlinear Gaussian-noise characteristic still provides an optimistic 1 dBc point. To take this into account, the total distortion power and power to distortion (P/D) (Refs. 15 and 16) have been obtained by simulation and measurement. These characteristics give a very accurate idea of the amplifier linearity as a function of the input power.

The paper is organized as follows. In Sec. II, a simple analytical study of the nonlinear behavior of amplifiers when excited with multitone signals is described. In Sec. III, nonlinear characteristics and figures of merit, with multitone and Gaussian-noise excitation signals, are obtained by simulation

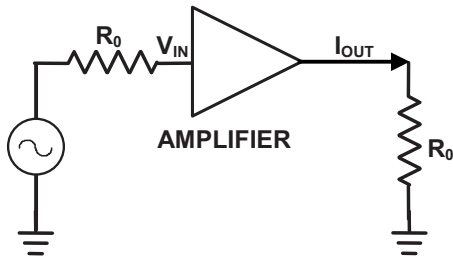


FIG. 1. Schematic of the amplifier example.

of a behavioral model of the particular LNA reported in the work and also by measurement. Finally, conclusions are summarized in Sec. IV.

II. NONLINEARITY ANALYTICAL STUDY OF AMPLIFIERS

This section describes a simple analytical study of the compression effects in amplifiers as a function of the number of tones of the excitation signal. For a more detailed analysis, see Ref. 17.

Figure 1 shows the schematic of a generic amplifier with a multitone voltage excitation signal and a load resistance of value R_0 . For simplicity the input impedance of the amplifier is also R_0 . On the other hand, the output current of the amplifier I_{out} is a function of the input voltage V_{in} and is given analytically by

$$I_{out} = a_1 \cdot V_{in} + a_3 \cdot (V_{in})^3. \quad (1)$$

We suppose that the coefficients a_1 and a_3 are real, so, in order to simplify the calculations, the equation corresponds to a memoryless weakly nonlinear amplifier. By means of simple mathematical developments, it is possible to conclude that for a generic N -tone excitation signal in the form of

$$V_{in} = \frac{V}{\sqrt{N}} \cdot \sum_{i=1}^N [\cos(\omega_i \cdot t)], \quad (2)$$

which has been the input power,

$$\overline{P_{in}} = \frac{V^2}{2 \cdot R_0}, \quad (3)$$

the analytical expression of the nonlinear characteristic turns out to be

$$\begin{aligned} \overline{P_{out}}_{\omega_1, \dots, \omega_N} = & (R_0^2 \cdot a_1^2) \cdot \overline{P_{in}} \\ & + \left(\left[6 - \left(\frac{3}{N} \right) \right] \cdot R_0^3 \cdot a_1 \cdot a_3 \right) \cdot \overline{P_{in}}^2 \\ & + \left(\left[9 \cdot \left(1 - \frac{1}{2 \cdot N} \right)^2 \right] \cdot R_0^4 \cdot a_3^2 \right) \cdot \overline{P_{in}}^3. \end{aligned} \quad (4)$$

The nonlinear terms of the previous equation are higher when the number of tones is increased, so we can deduce that the amplifier's AM-AM characteristic becomes more nonlinear. On the other hand, the linear term of the amplifier gain is not altered.

Let us define the following coefficients:

TABLE I. Summary of coefficient values.

N	C_2	C_3
1	3	9/4
2	9/2	81/16
3	5	25/4
4	21/4	441/64
∞	6	9

$$C_2(N) = 6 - (3/N),$$

$$C_3(N) = 9 \cdot \{1 - [1/(2 \cdot N)]\}^2.$$

(5)

In Table I the values of C_2 and C_3 as a function of the input signal's number of tones are summarized.

As we have previously mentioned, the paper is focused on one LNA, in particular, the Avago Technologies AMMC-6241, to illustrate the work. The typical one-tone AM-AM characteristic has been measured, obtaining a linear gain of 17.4 dB and a 1 dBc point with -10 dBm of input power and 6.4 dBm of output power. The analytical model parameters fitting the gain and 1 dBc point are $R_0=50$, $a_1=0.1482621$, and $a_3=-2.1535$. The nonlinear effects produced by the multitone signals are shown in Fig. 2, where the nonlinear characteristics obtained when giving these particular values to R_0 , a_1 , and a_3 can be observed. From this figure, it can be observed that the higher the number of tones of the excitation signal is, the higher the nonlinearity of the amplifier appears to be. On the other hand, the 1 dBc tends to a limit point ($P_{in}=-13$ dBm) when having a sufficient high

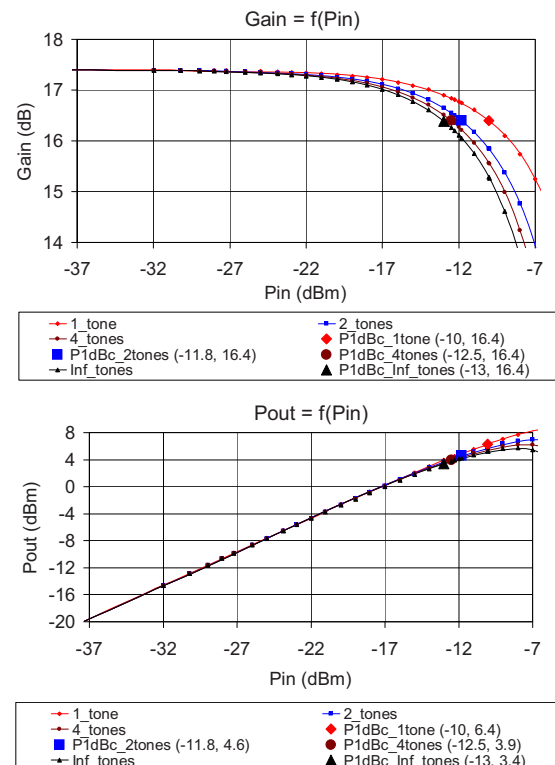


FIG. 2. (Color online) Nonlinear characteristics and 1 dBc points of the analytically modeled amplifier. Diamonds: single-tone excitation. Squares: two-tone excitation. Dots: four-tone excitation. Triangles: infinite-tone excitation.

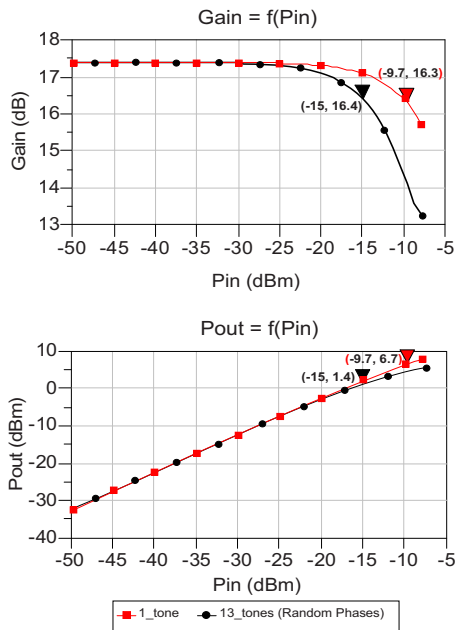


FIG. 3. (Color online) Nonlinear characteristics and 1 dBc points of the AMMC-6241 analytical model. Squares: single-tone excitation (31 GHz). Dots: 13 tone with random phase excitation signal.

number of tones. This apparent limit in the nonlinear compression has to be taken carefully. In the reported simplified development, the different tones are supposed to have phase equal to zero all of them. However, an equivalent “Gaussian-noise signal” has to be composed of several tones with random phases at different frequencies, covering the bandwidth of interest.

The analytical model of Fig. 1 has been implemented in the commercial software ADS of Agilent Technologies. In Fig. 3 the AM-AM characteristics have been achieved simulating with such an equivalent Gaussian-noise signal composed by 13 tones with random phases and also with the single-tone one. The 1 dBc point has an input power of -15 dBm, which is 2 dB lower than the limit point in Fig. 2. The real input signal to a LNA with astronomical applications is a wide-band Gaussian-noise signal that can be considered as a multitone signal composed of an infinite number of tones with random phases, so it would appear to be reasonable to expect a similar compression to that in Fig. 3.

III. AMMC-6241 SIMULATED AND MEASURED NONLINEAR CHARACTERISTICS

In Sec. II, a simplified analytical model of one of the QUIJOTE radiometer LNAs has been used to predict its nonlinear behavior with multitone excitation signals. In this section a more detailed behavioral model of the LNA is simulated to obtain more realistic nonlinear characteristics and also measurement results are shown.

A. AMMC-6241 behavioral modeling

A Wiener type model has been used for the reported LNA.¹⁸ This kind of model is suitable for weak or strong nonlinearities with memory. It consists of the series connection of a simplified equivalent electric circuit, reproducing

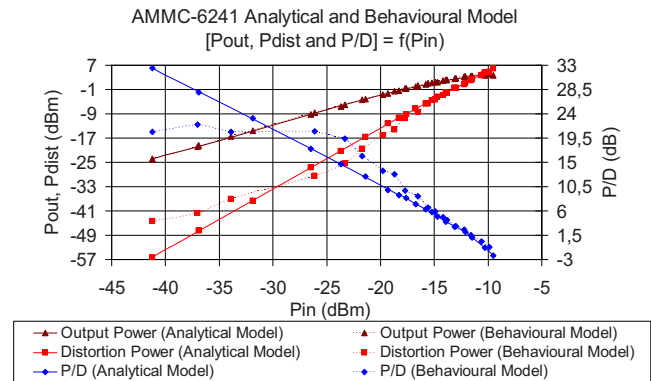


FIG. 4. (Color online) Output power (triangles), distortion power (squares), and P/D (diamonds) achieved by the simulation of the analytical model (solid lines) and the measurement-based behavioral model (dashed lines) with Gaussian-noise excitation signals.

the small-signal memory of the amplifier, and a memoryless nonlinearity implementing the single tone AM-AM nonlinear characteristic measured up to a high degree of compression. The memoryless block can be implemented by means of specific library elements available in any commercial simulator. The small-signal behavior of the nonlinear block has to accomplish perfect matching ($S_{ii}=0$) and perfect and bilateral transmission ($S_{ij}=1$), independent of the frequency. By this way, the matching conditions will be determined by the linear filter characterizing the linear dynamics, affected, in turn, by the nonlinear AM-AM characteristic. The model does not suffer from convergence problems and allows accurate nonlinear time-domain simulation, which is essential when the input signal is Gaussian white noise, with continuous spectra, as is the case of radiometric receivers. The linear filter is obtained by the application of linear system modeling techniques,¹⁹ obtaining an equivalent lumped-element filter with the same frequency response than obtained by measuring the $[S]$ parameters of the amplifier.

B. Measurement-based model simulation

The previously reported behavioral model is more accurate than the analytical one of Sec. II because it fits exactly the measured memoryless nonlinear AM-AM characteristic, and also because it characterizes the linear distortion corresponding to the small-signal memory effects. In order to show the differences between both types of models let us introduce the concept of distortion power and P/D ratio for an amplifier. The distortion power is the difference between the output power of a purely linear amplifier and the output power of the corresponding nonlinear amplifier in decibels. On the other hand, the P/D ratio is the ratio between the output power of the nonlinear amplifier and the corresponding distortion power in decibels.

Figure 4 shows the output power (triangles), the distortion power (squares), and the P/D (diamonds) achieved by the simulation of the analytical model (solid lines) and the measurement-based behavioral model (dashed lines) with Gaussian-noise excitation signals, simulated by means of pass-band filtered white-noise signals.¹² The band of the signals extends from 26 to 36 GHz. In this figure, there can be distinguished three regions. The first region is the smallest

signal region, from -42 to -30 dBm of input power, where the analytical model shows lower distortion than the behavioral one. This is because the analytical model's small signal behavior is defined by a real gain with no dependence on frequency, so there is no linear distortion, and the total distortion tends to zero when input power is near zero. Nevertheless, the behavioral model characterizes the linear distortion, given by the small-signal frequency response of the model, which presents a characteristic proportional to the output power in this smallest-signal region (see graph's triangles and squares). In this region it is possible to assume that the amplifier behavior is almost linear. In the second region, from -30 to -15 dBm of input power, the behavioral model presents lower distortion than the analytical one. This is because the analytical model's nonlinear behavior is defined only by quadratic and cubic polynomial terms [see Eq. (3)], while the nonlinear characteristic of the behavioral model fits the measured one with higher-order polynomial terms. These higher-order terms have the effect of smooth nonlinearity and, in consequence, the distortion in the reported region of the nonlinear characteristics. Finally, in the third region, from -15 to -10 dBm, the distortion generated by both models is very similar, because in this region the cubic polynomial term characterizes quite accurately the nonlinear behavior of the amplifier.

The nonlinear characteristics of the behavioral model, in form of Gain and Pin-Pout, have been also achieved by simulation and compared with the measured ones. The results are compared in Sec. III D.

C. Measurement set-up

The following is devoted to the validation of previous results by measurement of the AMMC-6241 AM-AM and distortion characteristics in the laboratory. The LNA excitations have been one and two-tone signals and also filtered Gaussian-noise signals. The reported amplifier is a commercial monolithic LNA that is manufactured using a pseudo-morphic high-electron mobility transistor process.

Two different set-ups were employed: the first one using sinusoidal continuous waves as input signals and the second one injecting wide-band noise to the amplifier. A synthesized sweep generator HP83650B was used to provide a single tone stimulus to the amplifier. For the two-tone test an additional synthesized sweep generator was added, combining both signals with a directional coupler in waveguide WR28 with a 3 dB coupling factor. The input signal was monitored on a spectrum analyzer E4446A to fix equal power levels in both tones, prior to apply them to the amplifier.

The second set-up was intended to provide a noisy wide-band signal in the operation bandwidth of the amplifier with a power level high enough to allow sweeping the power entering the amplifier using a rotating waveguide attenuator. A R347B noise source with 12 dB of excess noise ratio was used to provide the noisy signal. To reach the required power in the band of interest, two available gain-filtering blocks covering the 26–33 GHz band were cascaded at the source. Power budget calculations were performed to assure that the rotating attenuator placed in-between both blocks prevents nonlinear distortion in the second block. Anyway, both de-

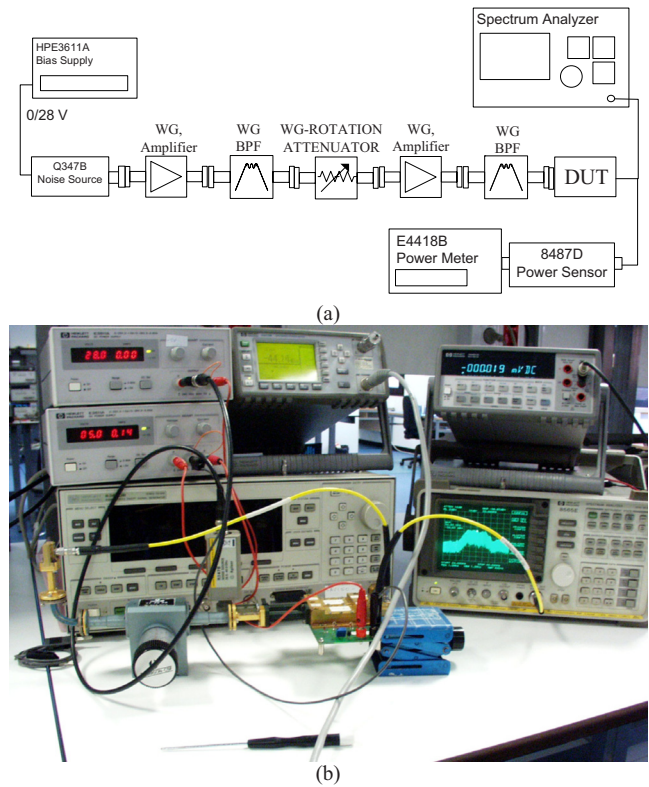


FIG. 5. (Color online) Block diagram (a) and photograph (b) of the measurement set-up with noisy wide-band excitation signal.

vice under test (DUT) input and output signals were measured for each power level, so the DUT nonlinear characteristic is obtained from measurements. An HP-E4418B power meter was used to measure total power without discrimination of frequencies and validate measurements on the spectrum analyzer, especially with the noisy wide-band signal. Figure 5 shows the block diagram (a) and a photograph (b) of the measurement set-up to generate a noisy wide-band signal as excitation for the LNA. In Fig. 5(b) it is also possible to appreciate the spectrum of the wide-band noise excitation signal.

D. Measurements results

Figure 6 compares the nonlinear characteristics of the LNA measured (triangles, squares, and diamonds) and simulated (solid lines) using the behavioral model. The results prove the accuracy of the behavioral model. The reported 1 dBc point with Gaussian-noise excitation signals has an input power of -15.1 dBm, which is 5 dB lower than obtained with a single-tone signal and corresponds almost exactly to the 1 dBc point in Fig. 3. Nevertheless, these results do not show clearly the real distortion that is produced when using such excitation signals, so the distortion and power to distortion characteristics have been achieved to clarify this point by means of measurement results. Input and output measured spectra and measured S parameters in linear operation were employed.

Figure 7 shows the output power (triangles), the distortion power (squares), and the P/D (diamonds) achieved by the measurement (solid lines) and the simulation of the be-

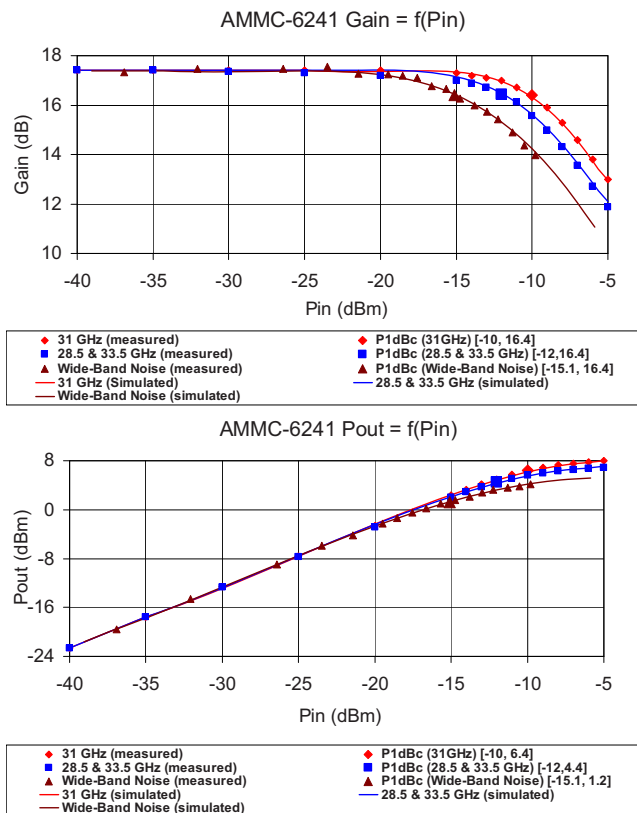


FIG. 6. (Color online) Measured nonlinear characteristics and 1 dBc points of the AMMC-6241 LNA. Diamonds: single-tone excitation (31 GHz). Squares: two-tone excitation (28.5 and 33.5 GHz). Triangles: filtered Gaussian noise.

havioral model (dashed lines). Also three reference points have been selected as representatives of the linear operation (a), the nonlinear operation in the 1 dBc point (b), and strongly nonlinear operation (c). It can be observed that measurement and simulation results are very similar.

Figure 8 shows the measured frequency-spectra of the output power and the distortion power in the reference points in Fig. 7. The output spectra have been achieved directly by measurement [see Fig. 5(b)]. Distortion spectra have been achieved indirectly by means of measured linear S param-

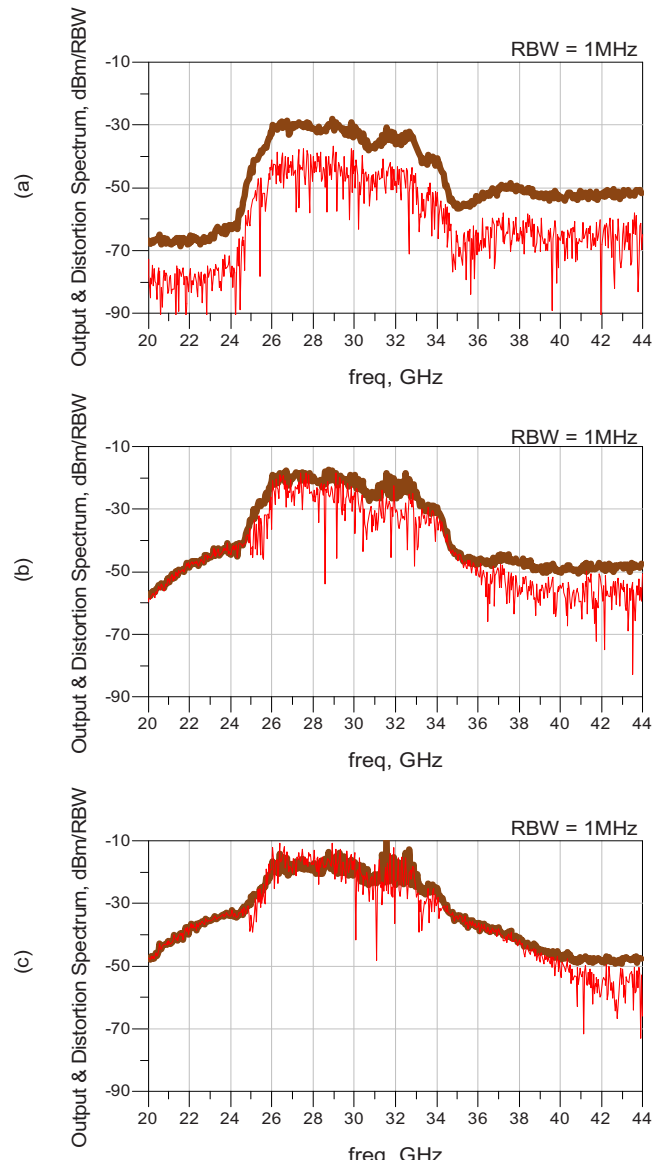


FIG. 8. (Color online) Measured output and distortion spectra with a resolution bandwidth, RBW=1 MHz, in the reported reference points. (a) Linear operation. (b) 1 dBc point operation. (c) Strongly nonlinear operation.

eters. We have used as excitation signal the measured input signals, and the distortion spectra have been achieved by subtraction of the linear model's output spectra, in watts, to the measured one. In (a) the output power is -9 dBm and the distortion power is -28 dBm. On the other hand, it can be observed how, in the 1 dBc point (b), a big part of the output signal (1.5 dBm) is generated by distortion (-3.7 dBm), while in the strongly nonlinear operation point the distortion power (5 dBm) is even higher than the output power (4.2 dBm) due to the high compression degree achieved in this point.

Taking into account the reported results, a good design rule to ensure the linearity in the operation of a LNA for astronomical applications is to set the required input back-off, with respect to the single-tone 1 dBc point, to assure that the LNA is operating at power levels where the only distortion generated by the amplifier is the amplitude and phase-distortion caused by the linear memory effects, but any non-

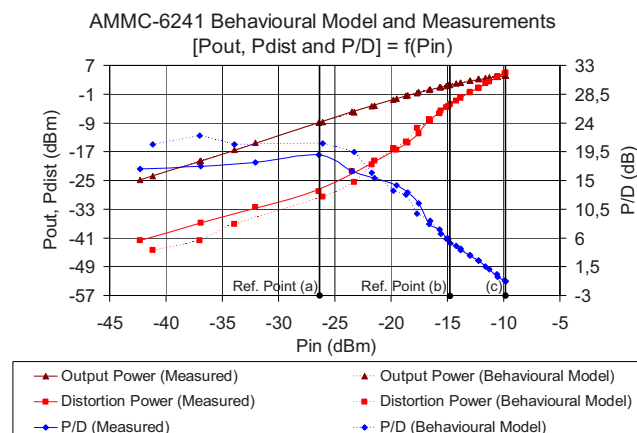


FIG. 7. (Color online) Output power (triangles), distortion power (squares), and P/D (diamonds) achieved by the measurement (solid lines) and the simulation of the behavioral model (dashed lines) with Gaussian-noise excitation signals.

linear distortion is produced. These power levels can be identified in Fig. 7 by the region where the distortion power is linearly proportional to the output power (P/D is almost constant). This region has a maximum input power of approximately -25 dBm, so in the reported case, at least a 15 dB input back-off with respect to the single-tone 1 dBc point has to be set. For the AMMC-6241, the expected input power to the QUIJOTE experiment BEM is around -53 dBm, so the linearity is clearly established.

IV. CONCLUSION

This paper shows the effects of wide-band Gaussian-noise excitation signals on the nonlinear behavior of LNAs employed in radiometers and instruments with astronomical applications. The use of multitone excitation signals, as a first approximation to a wide-band signal, and also filtered Gaussian noise has shown that the typical single-tone 1 dBc point is not appropriate as a linearity indicator in the instrument designing process.

The work has been focused on a particular LNA used in the BEM for the 31 GHz receiver of the QUIJOTE experiment radiometer. Taking into account a Gaussian-noise excitation signal in the working band of this receiver, from 26 to 36 GHz, the resulting 1 dBc point has an input power around 5 dB lower than the one corresponding to the single-tone 1 dBc point. In fact, the reported Gaussian-noise 1 dBc point is also optimistic due to the distortion that is added to the output power. Taking into account total distortion power and P/D ratio evaluation, it has been shown how a good design rule to apply in these cases consists of establishing the required input back-off, with respect to the single-tone 1 dBc point, to assure that the LNA is operating at power levels, where the only distortion generated by the amplifier is the linear memory distortion, so P/D has no dependence on input power. In our particular case, this rule makes us set at least a 15 dB input back-off with respect to the single-tone 1 dBc point.

It is also important to note the general applicability of the reported nonlinear study to all kinds of amplifiers and not only to LNAs. In the design processes of current communication transmitters and receivers, these effects also have to be taken into account, as they work with wide-band modulated signals.

In order to obtain a good idea about the linearity of an overall radio astronomy receiver, the following research line concerns the effects of the reported excitation signals in the nonlinearity of radiometric detectors.

ACKNOWLEDGMENTS

F.J.C. would like to acknowledge the financial support of the Spanish Science and Innovation Ministry (Project No. AYA2007-68058-C03-02) and program "Personal Técnico de Apoyo." J.P.P. acknowledges the financial support of the Spanish Science and Innovation Ministry (Project Nos. AYA2007-68058-C03-03 and TEC2008-06874-C03-01) and CONSOLIDER-INGENIO 2010 (Project No. CSD2008-00068). J.P. would like to acknowledge the financial support of the Spanish Science and Education Ministry (Project No. TEC2006-11077-C02-01).

The authors would like to express their gratitude to Dr. Reyes Ruiz for her help with mathematical expressions.

- ¹M. E. Tiuri, *IEEE Trans. Antennas Propag.* **AP-11**, 930 (1964).
- ²N. Skou, Proceedings of IGARSS, 2002, Vol. 6.
- ³M. Trier, IEEE IMTC Conference Record, 1993.
- ⁴F. Torres, I. Corbella, A. Camps, N. Duffo, M. Vall-Ilossera, S. Beraza, C. Gutierrez, and M. Martin-Neira, *IEEE Trans. Geosci. Remote Sens.* **44**, 2679 (2006).
- ⁵A. Colliander, L. Ruokokoski, J. Suomela, K. Veijola, J. Kettunen, V. Kangas, A. Aalto, M. Levander, H. Greus, M. T. Hallikainen, and J. Lahtinen, *IEEE Trans. Geosci. Remote Sens.* **45**, 7 (2007).
- ⁶V. S. Reinhardt, Y. Chi Shih, P. A. Toth, S. C. Reynolds, and A. L. Berman, *IEEE Trans. Microwave Theory Tech.* **43**, 715 (1995).
- ⁷T. Närhi, *Electron. Lett.* **32**, 224 (1996).
- ⁸C. A. Hoer, K. C. Roe, and C. M. Allred, *IEEE Trans. Instrum. Meas.* **IM-25**, 324 (1976).
- ⁹F. Torres, N. Duffo, I. Corbella, A. Camps, M. Vall-Ilossera, and L. Sagués, *Electron. Lett.* **39**, 1852 (2003).
- ¹⁰F. Torres, N. Duffo, C. Gonzalez-Haro, R. Vilaseca, L. Sagues, and M. Martin-Neira, IEEE IGARSS 2008, 2008, Vol. 2.
- ¹¹J. R. Piepmeier, P. N. Mohammed, and J. J. Knuble, *IEEE Trans. Geosci. Remote Sens.* **46**, 2 (2008).
- ¹²F. J. Casas, J. P. Pascual, J. Portilla, M. L. de la Fuente, B. Aja, and E. Artal, Eighth WSEAS International Conference on SSIP'08, 2008, pp. 107–111.
- ¹³G. N. Nkondem, J. Santiago, G. Neveux, D. Barataud, J. Collantes, J. Portilla, J. Nebus, and A. Mallet, IEEE MTT-S International Microwave Symposium Digest, 2008, pp. 1581–1584.
- ¹⁴J. A. Rubiño-Martín, R. Rebol, M. Tucci, R. Génova-Santos, S. R. Hildebrandt, R. Hoyland, J. M. Herreros, F. Gómez-Reñasco, C. López Carballo, E. Martínez-González, P. Vielva, D. Herranz, F. J. Casas, E. Artal, B. Aja, L. de la Fuente, J. L. Cano, E. Villa, A. Mediavilla, J. P. Pascual, L. Piccirillo, B. Maffei, G. Pisano, R. A. Watson, R. Davis, R. Davies, R. Battye, R. Saunders, K. Grainge, P. Scott, M. Hobson, A. Lasenby, G. Murga, C. Gómez, A. Gómez, J. Ariño, R. Sanquirc, J. Pan, A. Vizcargüenaga, and B. Etxeita, e-print arXiv:0810.3141v1.
- ¹⁵K. M. Gharaibeh, K. G. Gard, and M. B. Steer, IEEE Radio Wireless Symposium, 2006, pp. 487–490.
- ¹⁶J. C. Pedro and N. B. de Carvalho, *IEEE Trans. Microwave Theory Tech.* **47**, 2393 (1999).
- ¹⁷R. J. Westcott, *Proc. IEE* **114**, 726 (1967).
- ¹⁸K. M. C. Jeruchim, P. Balaban, and K. S. Shanmugan, *Simulation of Communication Systems* (Kluwer Academic/Plenum, New York, 2000).
- ¹⁹F. J. Casas, J. Portilla, R. Quere, A. Mallet, and J. F. Villemazet, *IEEE Trans. Microwave Theory Tech.* **52**, 2262 (2004).